Laboratory Investigation (2010) 90, 374–382

TIMP-2 modulates VEGFR-2 phosphorylation and enhances phosphodiesterase activity in endothelial cells

Seo-Jin Lee[1,3], Patricia S Tsang[2], Tere M Diaz[1], Bei-yang Wei[1] and William George Stetler-Stevenson[1]

In this study, we examine the effects of tissue inhibitor of metalloproteinases-2 (TIMP-2) on the phosphorylation status of specific phosphotyrosine residues on the vascular endothelial cell growth factor receptor-2 (VEGFR-2) cytoplasmic tail and examine the effects on associated downstream signaling pathways. To focus on metalloproteinase-independent mechanisms, we used the TIMP-2 analog known as Ala + TIMP-2 that is deficient in matrix metalloproteinase-inhibitory activity. Our experiments are designed to compare the effects of VEGF-A stimulation with or without Ala + TIMP-2 pretreatment, as well as basal responses in human microvascular endothelial cells. Our results show that Ala + TIMP-2 selectively alters the phosphorylation pattern of VEGFR-2 after VEGF-A stimulation and disrupts the downstream activation of PLC-γ, Ca^{+2} flux, Akt, and eNOS, as well as decreasing cGMP levels. Moreover, we observed an Ala + TIMP-2-induced reduction in cGMP levels typically elevated by exogenous NO donors implicating Ala + TIMP-2 in the direct activation of an isobutylmethylxanthine (IBMX)-sensitive cGMP phosphodiesterase activity. TIMP-2 suppression of endothelial mitogenesis and angiogenesis involves at least two mechanisms, one mediated by protein tyrosine phosphatase inhibition of VEGFR-2 activation as well as downstream signaling and a second mechanism involving direct activation of an IBMX-sensitive phosphodiesterase activity.

Laboratory Investigation (2010) **90,** 374–382; doi:10.1038/labinvest.2009.136; published online 18 January 2010

KEYWORDS: angiogenesis; endothelial cells; protein tyrosine phosphatase; phosphodiesterase; tissue inhibitors of metalloproteinases

Tumor angiogenesis is initiated by the hypoxic conditions related to rapid tumor growth that initiates tumor cell transcriptional activation of vascular endothelial growth factor (VEGF)-A.[1] Tumor progression is also associated with remodeling of the extracellular matrix by members of the matrix metalloproteinase (MMP) family and concomitant release of proteolytic cleavage products of laminin, fibronectin, and collagens, as well as sequestered growth factors including VEGF-A.[2,3] VEGF-A is well characterized as a potent inducer of endothelial cell proliferation, migration, and survival associated with tumor progression.

Vascular endothelial growth factor receptor-2 (VEGFR-2) signaling is critical for the angiogenic response associated with cancer progression. The central role of the VEGF-A/VEGFR-2 receptor axis in pathologic angiogenesis is reflected in the development of multiple Federal Drug Administration approved human therapeutic strategies that selectively target VEGF-A/VEGFR-2. For example, Bevacisumab and Sunitinib are approved for cancer treatment, as well as Pegaptanib and Ranibizumad for treatment of patients with macular degeneration, and several other drugs are now in late stage clinical trials.[4–6]

Similar to other receptor tyrosine kinases (RTKs) activation of VEGFR-2 signaling begins with ligand binding that results in receptor dimerization and autophosphorylation of specific tyrosine residues.[2,7] Phosphorylation of specific tyrosine residues is essential for the recruitment and activation of Src-homolgy-2 (SH2) binding proteins that propagate downstream intracellular signaling pathways. VEGFR-2 initiated signaling pathways regulate endothelial cell proliferation, migration, survival and vascular permeability.

Mammalian tissue inhibitor of metalloproteinases (TIMPs) are a family of four relatively small proteins that contain six disulfide bonds.[8] TIMP-2 is unique in that, it is the only member of the family that functions to both inhibit MMP activity, and facilitate the cell surface activation of pro-MMP-2 through formation of a tri-molecular complex with MT1-MMP.[8] In addition, TIMP-2 is the only TIMP family

[1]Radiation Oncology Branch, Center for Cancer Research, National Cancer Institute, Bethesda, MD, USA and [2]Pediatric Oncology Branch, National Cancer Institute, Bethesda, MD, USA
Correspondence: Dr WG Stetler-Stevenson, MD, PhD, Radiation Oncology Branch, CCR, NCI, Advanced Technology Center, 8717 Grovemont Circle, Room 115, Bethesda, MD 20892-4605, USA.
E-mail: sstevenw@mail.nih.gov
[3]Current address: Shingyeong University, Room 206, Namyang-dong, Hwaseong-si, Gyeonggi-do, Republic of Korea 445-741.

Received 27 August 2009; revised 19 October 2009; accepted 16 November 2009

member that is a potent inhibitor of human microvascular endothelial cell (hMVEC) mitogenesis *in vitro* and angiogenesis *in vivo*, and these effects are independent of MMP-inhibitory activity, as shown by the TIMP-2 analog, Ala + TIMP-2 that is devoid of MMP-inhibitory activity.[9–12] The anti-angiogenic effect of TIMP-2 and Ala + TIMP-2 involves heterologous receptor inactivation. The specific mechanism involves binding of TIMP-2 or Ala + TIMP-2 to the $\alpha 3\beta 1$ integrin, induction of protein tyrosine phosphatase (PTP) activity, and subsequent reduction in activation/phosphorylation of angiogenic RTKs, such as VEGFR-2 and FGFR-1.[10–12] Furthermore, studies using mice 80–90% deficient in Shp-1 show that the *in vivo* anti-angiogenic activity of Ala + TIMP-2 is dependent on Shp-1 activity.[13] In addition to inhibition of endothelial cell mitogenesis TIMP-2 inhibits endothelial cell migration, also via an Shp-1-dependent mechanism.[14]

On the basis of our previous demonstration that all TIMP-2 and Ala + TIMP-2 effects are Shp-1 dependent, we have not repeated these experiments here but choose to further our understanding of the anti-angiogenic mechanism of TIMP-2 through examining the effects on the pattern of VEGFR-2 phosphorylation in the cytoplasmic tail. To focus on MMP-independent effects of TIMP-2 experiments were conducted using the TIMP-2 analog, which we refer to as Ala + TIMP-2 that is deficient in MMP-inhibitory activity.[15] We show for the first time that Ala + TIMP-2 selectively alters VEGFR-2 phosphorylation, and diminished VEGF-A-mediated activation of downstream effectors. Also for the first time, we observed that elevation of cGMP levels by administration of exogenous NO donors was directly down-regulated by Ala + TIMP-2 through induction of isobutyl-methylxanthine (IBMX)-sensitive phosphodiesterase activity. These findings extend previous observations of the inhibitory effects of extracellular matrix proteins, specifically TIMP-2, on the proliferation and migration of hMVECs and provide novel insight into extracellular matrix regulatory signals that modulate cellular responses to VEGF-A.

MATERIALS AND METHODS

Cell Lines, Growth Factors, Antibodies, and Reagents

Primary hMVECs and growth factors were purchased from commercial sources. Primary hMVECs were used between passages 3 and 6 for all experiments as described earlier.[11] Antibodies recognizing VEGFR-2 phosphorylated tyrosine residues: pY^{951}, pY^{1059}, and pY^{1214} were purchased from Biosource (Invitrogen, Carlsbad, CA, USA); anti-pY^{996} and anti-pY^{1175} were from Cell Signaling Technology (Danvers, MA, USA). Anti-PLC-γ-pY^{783} and anti-PLC-γ antibodies were from Biosource. Anti-phosho-AKT (S^{473}), anti-AKT, anti-phospho-eNOS (S^{1177}), and anti-eNOS antibodies were purchased from Cell Signaling Technology. Anti-VEGFR-2 antibody was obtained from Santa Cruz Biotechnology (Santa Cruz, CA, USA).

Diethyltriamine NONOate (DETA/NO) and fura2-acetoxymethyl ester (fura-2, AM) were purchased from Cayman Chemical (Ann Arbor, MI, USA), and Molecular Probes (Invitrogen, Carlsbad, CA, USA), respectively. BAPTA-AM and 1H-(1,2,4) oxadiazole(4,3-a)quinoxalin-1-one (ODQ) were obtained from BIOMOL (Plymouth Meeting, PA, USA). Sodium orthovanadate, okadaic acid, 8-Bromo (8Br)-cGMP, 4,5-diaminofluorescein diacetate (DAF-2DA), N^{ω}-nitro-L-arginine methyl ester (L-NAME), and 3-isobutyl-1-metylxanthine (IBMX) were purchased from Sigma-Aldrich Chemical (St Louis, MO, USA). Recombinant TIMP-2 and Ala + TIMP-2 were prepared as described, and endotoxin tested using the Limulus amoebocyte lysis assay (< 2 EU/mg protein), as reported earlier.[15]

Cytosolic Ca^{2+} Measurement

Increases in intracellular Ca^{2+} were measured using the Ca^{2+}-sensitive fluorescent dye fura-2 AM using gelatin-coated 96-well black wall plates (BioCoat, BD Biosciences, San Jose, CA, USA). hMVECs were incubated with 4 μM fura-2 AM for 30 min at 37°C, gently washed twice with Hank's balanced salt solution (Invitrogen), and treated as indicated. The treated cells were then imaged using a BD Pathway 855 bioimager (BD Biosciences). Regions of interest in individual cells were gated and excited at 334 and 380 nM with emission at 520 nM. The 334/380-excitation ratio, which increases as a function of intracellular Ca^{2+} concentration, was captured at 4-s intervals.

Immunoblotting and Immunoprecipitation

After specified treatments, hMVECs were rinsed twice with ice-cold phosphate-buffered saline and lysed in buffer A (50 mM Tris-HCl, pH 7.4, 150 mM NaCl, 0.25% sodium deoxycholate, and 1% Triton X-100), supplemented with 1 mM EDTA, 1 mM phenylmethylsulfonyl fluoride, 1 μg/ml leupeptin, 1 μg/ml aprotinin, 1 μg/ml pepstatin, and 100 μM Na_3VO_4, for 20 min on ice. Insoluble material was removed by centrifugation at 4°C for 20 min at 14 000 r.p.m. Protein concentration in the lysates was determined with a BCA protein assay kit (Pierce, Rockford, IL, USA). To extract total eNOS protein, cells were lysed in buffer B containing SDS rather than Triton X-100 (50 mM Tris-HCl, pH 7.4, 2% SDS, 25 mM β-glycerophosphate, 50 mM NaF, and 0.5 mM Na_3VO_4). hMVECs lysates were subjected to immunoprecipitation and western blot analysis as described earlier.[16] Chemiluminescent generated band intensities were integrated for quantification by the use of National Institutes of Health (NIH) Image J 1.34s software.

Nitric Oxide Measurements

Total NO was assayed using nitrate/nitrite fluorometric assay kit from Cayman Chemical. hMVECs were washed with phenol-free basal media and incubated with TIMP-2 (50 nM), Ala + TIMP-2 (50 nM), or L-NAME (1 mM) in the absence of and presence of VEGF-A. The nitrite and

nitrate released into the media were measured fluorimetrically (excitation wavelength 355 nM: emission wavelength 460 nM), according to the manufacturer's instructions (Cayman Chemical).

Intracellular NO was measured using the NO-specific fluorescence probe DAF-2DA as described.[17] Total fluorescence of the treated and washed samples was determined (emission wavelength, 485 nM; excitation wavelength 538 nM) using the bottom-reading mode in a fluorescence plate reader (Tecan).

Intracellular cGMP Measurement

Intracellular cGMP concentrations were determined as described earlier.[18] The experimental readings from each triplicate lysates falling within the linear region of the standard curve were evaluated with the Direct cGMP Assay Kit from Assay Designs (Ann Arbor, MI, USA).

Cell Proliferation Assay

The number of hMVECs, after indicated *in vitro* treatments, were determined using Cell-Titer 96 Aqueous One Solution reagent (Promega) according to the manufacturer's direction, as described earlier.[11]

Cell Migration Assay

To assess cell migration, the 'scratch' wound assay was performed as described earlier and quantified by measuring the width of the cell-free zone immediately before and 16 h after cell treatment using a computer-assisted microscope (Zeiss) at three distinct positions for each assay condition. The results are reported as the mean ± s.d. of these triplicate measurements.

Statistical Analysis

All data were analyzed using the Prism Statistical Software package (Software MacKiev, Graphpad Software, La Jolla, CA, USA) to perform two-sided student *t*-test of statistical significance or ANOVA analysis.

RESULTS

TIMP-2 Shows Selective Inhibition of VEGFR-2 Tyrosine Phosphorylation

We have reported earlier that treatment of hMVECs with TIMP-2 results in a significant decrease in total VEGFR-2 tyrosine phosphorylation after VEGF-A stimulation,[11] resulting in complete inhibition of VEGF-A-stimulated mitogenesis. This effect is independent of the ability of TIMP-2 to inhibit MMP activity, as shown by the use of a TIMP-2 derivative devoid of MMP-inhibitory activity, Ala + TIMP-2. Furthermore, this effect was completely abrogated by the co-administration of the PTP-inhibitor sodium orthovanadate or genetic manipulation to reduce active Shp-1 levels.[11,12] To further elucidate the mechanisms through which TIMP-2 downregulates VEGF-A-mediated pro-angiogenic signaling, we examined the phosphorylation status of several tyrosine residues after treatment of hMVECs at 0, 2, 5, and 10 min after VEGF-A stimulation with or without previous Ala + TIMP-2 treatment, Figure 1. It is well recognized that VEGFR-2 phosphorylation is maximal between 2–5 min after VEGF-A stimulation and decreases thereafter.[19] Of the five tyrosine residues examined (Y^{951}, Y^{996}, Y^{1059}, Y^{1175}, and Y^{1214}) VEGF-A treatment alone showed enhanced phosphorylation of these residues that peaked at 5 min. Pretreatment of the hMVECs with 50 nM Ala + TIMP-2 for 30 min before VEGF-A stimulation resulted in minimal enhancement of Y^{1059} and Y^{1214} phosphorylation. These findings suggest that these residues are not targeted by the enhanced Shp-1 phosphatase activity previously observed after Ala + TIMP-2 pretreatment of VEGF-A-stimulated hMVECs.[11,12]

In contrast, Ala + TIMP-2 selectively suppressed maximal VEGF-A-stimulated phosphorylation of Y^{951}, Y^{996}, and Y^{1175} of the VEGFR-2 cytoplasmic domain and this effect peaked at 5 min after stimulation, Figure 1. These tyrosine residues have been specifically implicated in the regulation of hMVEC proliferation and migration, through initiation of critical downstream signaling pathways. Ala + TIMP-2 decreased phosphorylation of these specific tyrosine residues ranged from ~40% reduction for Y^{951} to ~50% reduction for both Y^{996} and Y^{1175}.

Zymogram analysis of MMP-2 expression revealed that Ala + TIMP-2 or TIMP-2 (50 or 100 nM final concentration) treatment of hMVECs failed to alter expression or activation of this MMP (data not shown).

TIMP-2 Inhibits PLC-γ Activation and Ca^{+2} Flux

As phosphorylation of Y^{951} and Y^{1175} are known to mediate activation of PLC-γ, we postulated that Ala + TIMP-2 reduction of phosphorylation at VEGFR-2 tyrosine residues Y^{951} and Y^{1175}, would decrease both PLC-γ activation and cytosolic Ca^{+2} concentrations. As shown in Figure 2a, hMVECs treated with 50 nM Ala + TIMP-2 before VEGF-A stimulation showed a significant (>65%) decrease in the association of PLC-γ with the VEGFR-2 at 5 min, as determined by immunoprecipitation analysis. We then examined the phosphorylation of PLC-γ on Y^{783} that has been associated with PLC-γ activation *in vitro* and *in vivo*.[20] At 2 min after treatment with VEGF-A, PLC-γ showed a ~9.0-fold increase in Y^{783} phosphorylation that was not significantly attenuated by TIMP-2 pretreatment, Figure 2b. However, at 5 min post-treatment PLC-γ activation as determined by Y^{783} phosphorylation was decreased by 40%. This observation suggest that Ala + TIMP-2 may not suppress maximal phosphorylation of PLC-γ at 2 min after VEGF-A stimulation, but does accelerate dephosphorylation as shown by reduced phosphorylation at both the 5 and 10 min time points. To further examine the effect of this apparent Ala + TIMP-2-mediated reduction in PLC-γ activation at 5 min, we measured cytosolic Ca^{+2} levels, which are normally increased in response to PLC-γ activation by

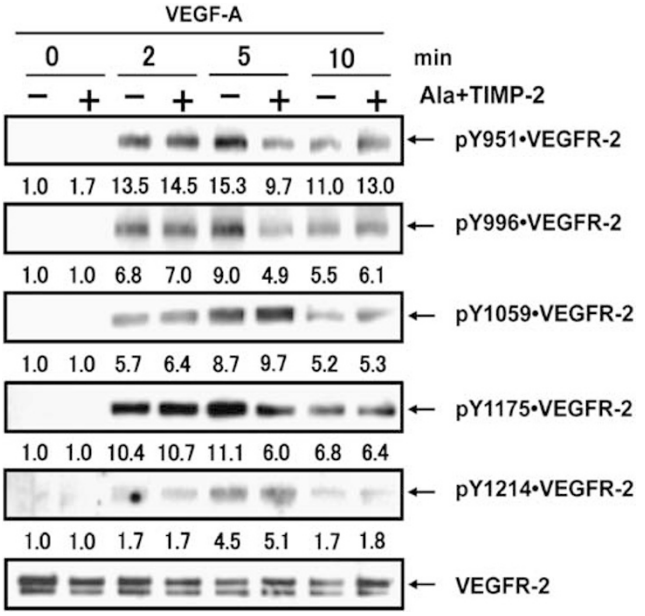

Figure 1 Ala + TIMP-2 suppresses VEGF-A-induced maximal phosphorylation of select tyrosine residues in VEGFR-2 in hMVECs. hMVECs stimulated with VEGF-A (10 ng/ml) for indicated time periods after pretreatment in the presence or absence of Ala + TIMP-2 (50 nM, 15 min) were subjected to western blot analysis with commercial antibodies. The western blots shown are representative of three independent experiments. Relative band intensities were measured by NIH image software and integrated densities were normalized against the VEGFR-2 loading control.

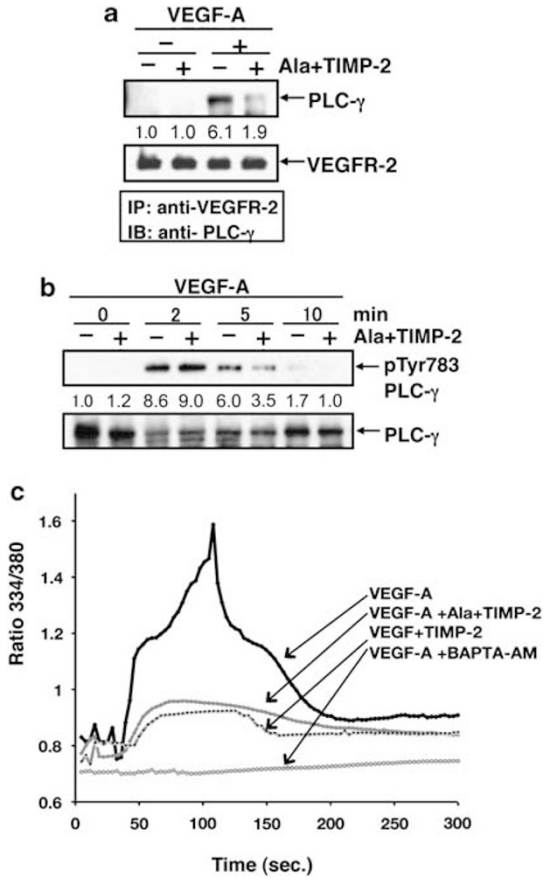

Figure 2 TIMP-2 accelerates VEGF-A-induced PLC-γ deactivation and suppresses intracellular Ca^{+2} influx. (**a**) hMVECs were treated with Ala + TIMP-2 (50 nM) before VEGF-A stimulation for 5 min. The cells were immediately rinsed and lysed as described in materials and methods. (**b**) hMVECs were stimulated with VEGF-A (10 ng/ml) in the absence or presence of Ala + TIMP-2 (50 nM) for the indicated time periods. Immunoblotting was performed using the antibody directed against pY^{783} PLC-γ and PLC-γ (loading control). Band intensities were integrated using NIH Image software and normalized using total PLC-γ at 0 min. Results are representative of three independent experiments. (**c**) Intracellular Ca^{2+} influx was measured using fura-2. hMVECs were treated with VEGF-A (10 ng/ml) in the absence or presence of Ala + TIMP-2 (50 nM), TIMP-2 (50 nM), or BAPTA-AM (10 μM). Specific cell treatments are indicated by arrows and legend. Each tracing is the average response of ~60 cells. Experiments were performed in triplicate and shown are representative tracings.

VEGFR-2.[21] Figure 2c shows that VEGF-A stimulation results in a significant biphasic Ca^{+2} flux that starts at ~60 s and shows a maximal response at 120 s, followed by a gradual return to baseline at 300 s. In contrast, 50 nM Ala + TIMP-2 or TIMP-2 treatment severely attenuates the initial phase of the Ca^{+2} flux that starts a 60 s and completely abrogates the Ca^{+2} spike that occurs around 120 s after VEGF-A treatment. The calcium-chelating agent, BAPTA-AM (negative control), suppressed both phases of the intracellular Ca^{+2} increase usually observed after VEGF-A stimulation. These results are consistent with the Ala + TIMP-2-mediated decreased association of PLC-γ with VEGFR-2 showed by co-immunoprecipitation experiments (Figure 2a), and decrease in PLC-γ phosphorylation/activation. In addition, these data also support the multiple modes of PLC-γ regulation and the recent observation that activation of PLC-γ requires overcoming auto-inhibition by the c-terminal SH2 domain, which is regulated by the split pleckstrin homology (sPHN) domain that occurs independently of Y^{783} phosphorylation.[22] Accordingly these findings may account for the apparent dissociation of PLC-γ phosphorylation/activation and the suppression of Ca^{+2} cytosolic flux between 2 and 5 min.

Ala + TIMP-2 Inhibits Phosphorylation/Activation of AKT and eNOS

Phosphorylation of Y^{1175} allows activation of the PI3K/AKT signaling pathway.[23] To assess the effect of Ala + TIMP-2-mediated reduction of Y^{1175} phosphorylation on downstream signaling via the PI3K/AKT pathway, we determined the level of AKT activation by assaying the phosphorylation status of serine 473 (S^{473}).[24] Ala + TIMP-2 significantly attenuated AKT phosphorylation on S^{473} at both 5 min (60% inhibition) and 10 min (40% inhibition) after VEGF-A stimulation (Figure 3a). The Ala + TIMP-2-mediated decrease in phosphorylation at this site was absent at the latter time point (30 min), further emphasizing the importance of suppressed AKT activation at the critical time point for activation of downstream pathways.

PLC-γ-associated intracellular Ca^{2+} flux is associated with calmodulin-mediated activation of eNOS,[25] but eNOS acti-

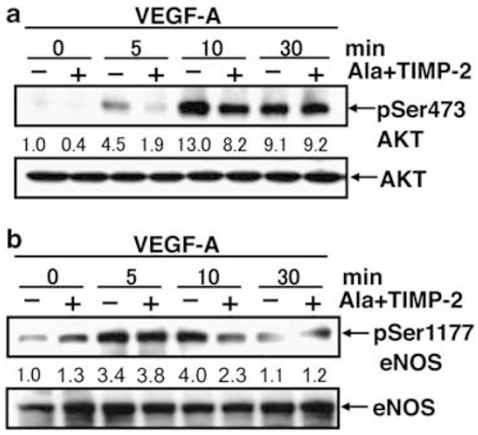

Figure 3 Ala + TIMP-2 suppresses Akt activation and maximal eNOS phosphorylation after VEGF-A stimulation. (**a**) hMVECs were stimulated with VEGF-A (10 ng/ml) in the absence or presence of Ala + TIMP-2 (50 nM) and cell lysates isolated at the indicated times after stimulation. The immunoblotting was performed using the antibodies against pS^{473} AKT and AKT. Band intensities were integrated using NIH Image software and normalized using total Akt at 0 min. Results shown are representative of three independent experiments. (**b**) The activation status of eNOS was evaluated by immuoblots of pS^{1177}eNOS. Band intensities were measured by NIH image software and normalized against total eNOS levels at time 0 min. Results shown are representative of three independent experiments.

vation may also be directly mediated by AKT phosphorylation of eNOS on S^{1177} in a Ca^{2+}-independent manner.[26] As we have shown earlier that TIMP-2 significantly suppresses the PLC-γ-mediated cytosolic Ca^{+2} flux, we evaluated eNOS activation status by examining S^{1177} phosphorylation status. VEGF-A-induced eNOS phosphorylation on S^{1177} was inhibited 40% by Ala + TIMP-2 at 10 min after stimulation (Figure 3b). As maximal VEGF-A-induced phosphorylation of S^{1177} was observed at 10 min, these data are consistent with the suppression of maximal eNOS activation at 10 min. Collectively, these findings are consistent with suppression of maximal VEGFR-2 phosphorylation on Y^{951}, and Y^{1175}, in response to Ala + TIMP-2 treatment, resulting in suppression of both the PLC-γ and PI3K/AKT signaling pathways, and are consistent with the observed downregulation of eNOS activation. These results led us to analyze NO and further downstream signaling after Ala + TIMP-2 treatment and VEGF-A stimulation of hMVECs.

TIMP-2 Inhibits VEGF-A-Induced NO Synthesis

Total NO levels were determined in VEGF-A-stimulated hMVEC in the absence or presence of TIMP-2, Ala + TIMP-2, or the NOS inhibitor L-NAME, Figure 4. VEGF-A evoked a twofold increase in total NO synthesis compared with basal conditions. In the presence of TIMP-2 or Ala + TIMP-2, we observed a statistically significant ($P<0.001$) inhibition of VEGF-A-stimulated total NO production close to basal levels and similar to those observed with L-NAME ($P<0.01$), Figure 4a. TIMP-2 and Ala + TIMP-2 both significantly reduced cytosolic NO levels close to basal levels ($P<0.001$), Figure 4b. The equipotent activity of TIMP-2 and Ala + TIMP-2 suggests that these effects were independent of MMP inhibition. These results are consistent with the reduced phosphorylation/activation of eNOS observed earlier (Figure 3b) and suggest that the 40% reduction in eNOS phosphorylation, combined with reduced cytosolic Ca^{+2} flux, are sufficient to reduce eNOS activity below the threshold level necessary for elevation of either total or cytosolic NO levels.

TIMP-2 Inhibits VEGF-A-Stimulated Increase in Cellular cGMP

Conformational changes resulting from NO binding to the sixth position of the heme ring of soluble guanylyl cyclase (sGC) leads to a 200-fold increase in activation of the enzyme, and subsequent increase in cytosolic cGMP levels.[27] In this study, we show that VEGF-A stimulation leads to a maximal fourfold increase in cGMP synthesis at 10 min, Figure 5a. Alternatively, in the presence of 50 nM concentrations of Ala + TIMP-2 (or TIMP-2), the normal VEGF-A-induced cGMP increase was suppressed to levels similar to those observed in the presence of the eNOS inhibitor L-NAME, Figure 5a. The suppression of cGMP production in the presence of Ala + TIMP-2, TIMP-2 and L-NAME are all statistically significant ($P<0.01$) at the 10 min time point, which was the point of maximal cGMP response to VEGF-A.

These findings are consistent with our previous observations that TIMP-2 or Ala + TIMP-2 decreased both VEGFR-2 phosphorylation and eNOS activity. We have shown earlier that the effects of TIMP-2 on hMVEC growth and migration are sensitive to the nonspecific PTP inhibitor orthovanadate (Na_3VO_4) and expression of dominant negative Shp1 (dnShp1).[11,12,28] Given that Okadaic acid suppresses the serine/threonine phosphatase activity of protein phosphatase 2a (PP2a) that modulates phosphorylation/activation of eNOS on S^{1177} we examined whether inhibition of either PTP or PP2a activities would reverse the TIMP-mediated suppression of VEGF-A-induced cGMP synthesis through alteration of VEGFR-2 or eNOS phosphorylation.[29] To this end, we determined the effects of both Na_3VO_4 and okadaic acid on cellular cGMP levels after VEGF-A stimulation with or without Ala + TIMP-2 treatment. Both orthovanadate and okadaic acid slightly inhibited VEGF-A-induced cGMP synthesis in hMVECs without TIMP-2 treatment, Figure 5b. However, the addition of either orthovanadate (1 μM) or okadaic acid (100 nM) cannot reverse the essentially complete suppression of VEGF-A-induced cGMP synthesis in hMVEC after Ala + TIMP-2 treatment, Figure 5b. These findings imply that the suppression of increased VEGF-A-induced cGMP levels observed after Ala + TIMP-2 treatment is not mediated solely via induction of Shp-1 or PP2a. Therefore, it is reasonable to assume that modulation of cGMP levels by Ala + TIMP-2 occurs through additional mechanisms that are independent of the Ala + TIMP-2-mediated decrease in VEGFR-2 phosphorylation and subsequent suppression of eNOS activation.

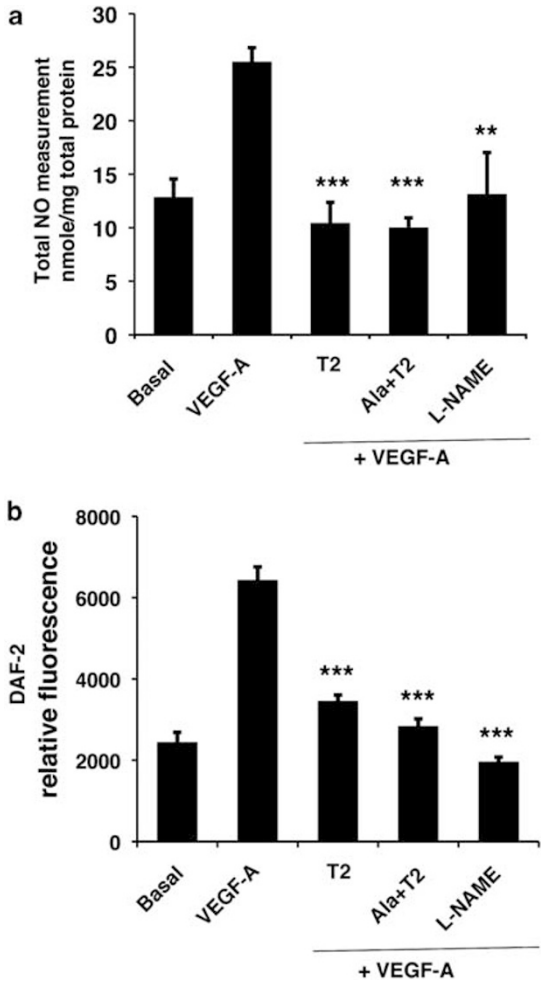

Figure 4 TIMP-2 restricts VEGF-A-mediated NO production. (**a**) hMVECs were incubated in the presence (+) or absence (Basal) of VEGF-A (10 ng/ml), as well as with VEGF-A after 15 min pretreatment with TIMP-2 (50 nM), Ala + TIMP-2 (50 nM), or L-NAME (1 mM) for 5 min. Total NO (nitrite and nitrate) released from cells in the medium was measured described in 'Materials and Methods section' and normalized for the amount of total cellular protein (mg). Data are expressed as mean ± s.d. of triplicate. $^{**}P<0.01$; $^{***}P<0.001$ *vs* VEGF-A treatment alone. (**b**) hMVECs were loaded with the fluorescent indicator DAF-2DA as described, and then treated as described in Figure 2a. Fluorescence was measured in a fluorescence plate reader. Data are expressed as mean ± s.d. of triplicate. $^{**}P<0.01$; $^{***}P<0.001$ *vs* VEGF-A treatment alone.

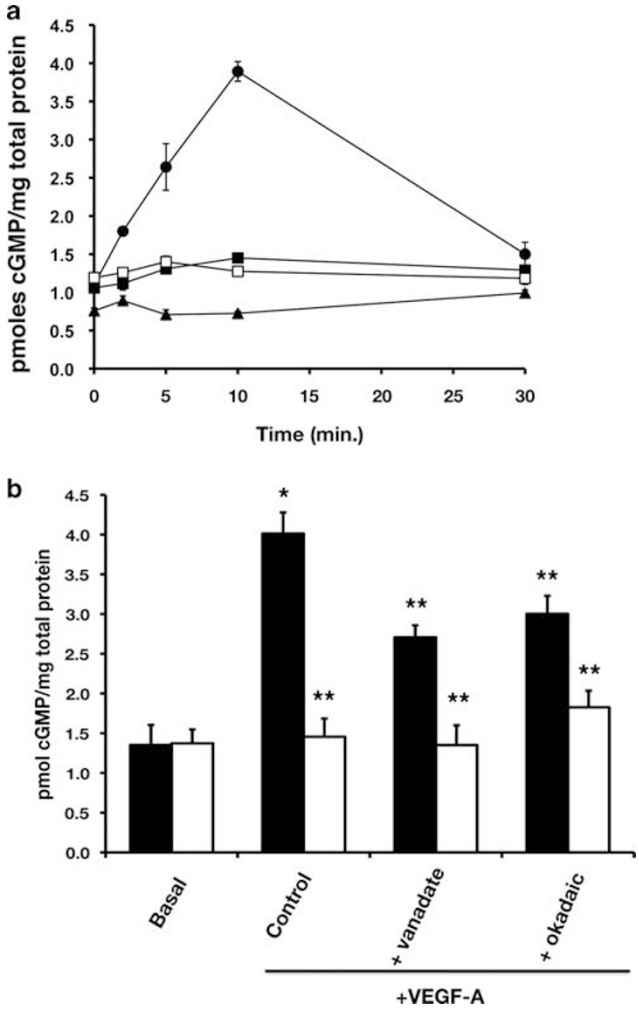

Figure 5 TIMP-2 inhibits cGMP synthesis evoked by VEGF-A leading to the inhibition of VEGF-A-induced cell proliferation and cell migration. (**a**) hMVECs were treated with VEGF-A for the indicated time course in the absence (solid circle) or presence of TIMP-2 (50 nM, solid square), Ala + TIMP-2 (50 nM, open square), or L-NAME (1 mM, solid triangle). The intracellular cGMP was determined as described in 'Materials and Methods section'. The data shown reflect the mean intracellular cGMP level from triplicates determinations and are representative of three independent experiments. (**b**) hMVECs were pretreated with either orthovanadate (1 μM) or okadaic acid (100 nM) for 30 min. and then stimulated with VEGF-A in the presence (black bars) or absence of Ala + TIMP-2 (white bars) for 10 min. The intracellular cGMP was determined as described in 'Materials and Methods section'. The shown data are the mean of intracellular cGMP level from triplicates determinations. $^{*}P<0.01$ *vs* control; $^{**}P<0.001$ *vs*VEGF-A alone in the absence of Ala + TIMP-2.

TIMP-2 Suppresses cGMP Production in Response to Exogenous NO Donors

To further examine this novel TIMP-2 signaling effect, we determined the ability of Ala + TIMP-2 to inhibit cGMP synthesis initiated by exogenous NO-donors. DETA/NO or SNAP are exogenous NO donors that can directly activate soluble guanylyl cyclase (sGC) and increase cytosolic cGMP levels.[30] Treatment of hMVECs with 10 μM of DETA/NO or SNAP for 5 min resulted in a significant increase in cGMP over basal levels, Figure 6a. DETA/NO gave ~5.5-fold increase, while SNAP gave a slightly lower, but still statistically significant ~3.5-fold increase over basal levels. Somewhat surprisingly, Ala + TIMP-2 (or TIMP-2) inhibited DETA/NO- or SNAP-induced cGMP synthesis in hMVECs in a statistically significant manner ($P<0.001$) comparable to levels observed with the selective guanylyl cyclase inhibitor ODQ (Figure 6a).

Previous studies show that NO effects on endothelial cell proliferation and migration are concentration dependent. DETA/NO at concentrations below 100 μM stimulate

proliferation and migration of endothelial cells, but inhibit these cellular responses at higher concentrations.[30] Similarly, treatment of hMVECs with 10 or 100 μM of DETA/NO or SNAP results in a two- to threefold increase in cell proliferation compared with basal levels. In this study, we show that Ala + TIMP-2 suppresses hMVEC proliferation after either 10 or 100 μmole/l of DETA/NO or SNAP in a statistically significant manner ($P<0.001$), Figure 6b. Although treatment with 10 μmole/l DETA/NO showed a twofold increase in spontaneous cell migration of hMVECs compared with basal migration, addition of Ala + TIMP-2 showed statistically significant inhibition of NO-stimulated cell migration at all concentrations tested, Figure 6c. In fact, Ala + TIMP-2 inhibited spontaneous hMVEC migration at 0 μM DETA/NO, consistent with out previous findings.[28]

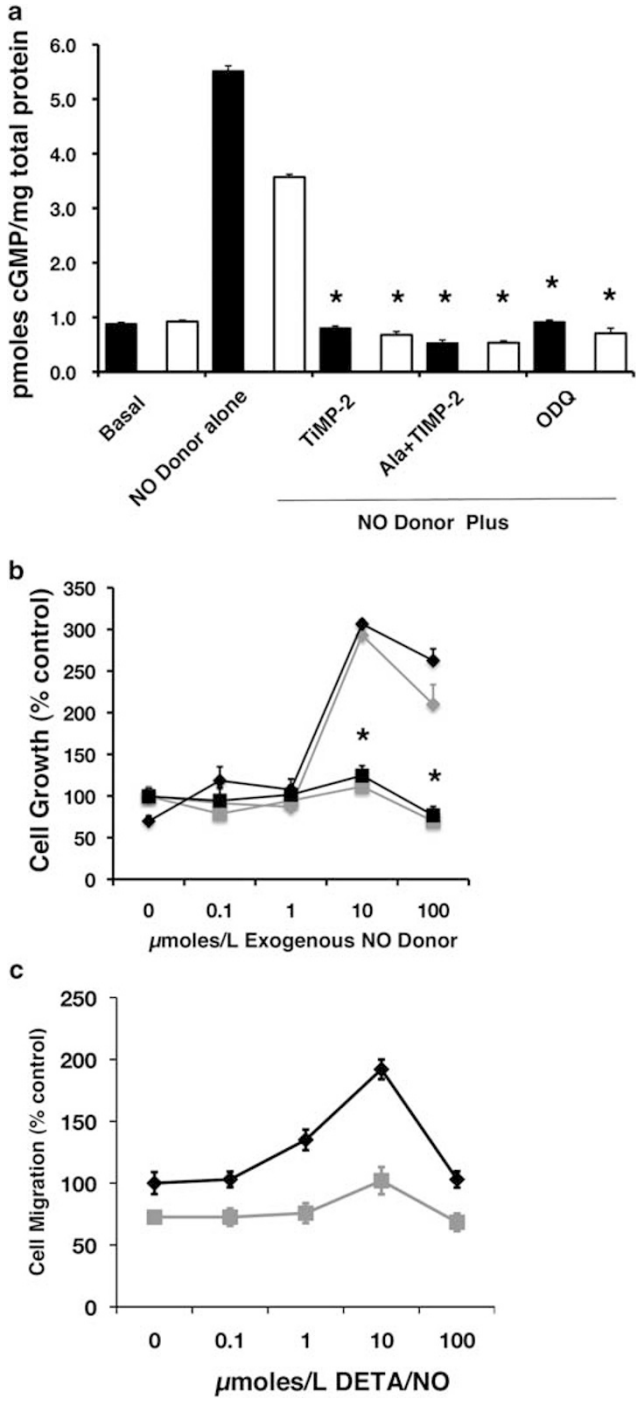

These studies show that Ala + TIMP-2 (or TIMP-2) directly downregulates exogenous NO donor-mediated increase in cGMP, as well as downstream suppression of cGMP-mediated increased hMVEC proliferation (DETA/NO and SNAP, Figure 6b) and migration DETA/NO, Figure 6c). It is possible that Ala + TIMP-2 (and TIMP-2) modulate cGMP levels by either suppressing sGC activity or enhancing phosphodiesterase (PDE) activity. Indeed, we showed that VEGF-A, Ala + TIMP-2 (and TIMP-2) suppress exogenous NO-induced hMVEC mitogenesis to near basal levels (Figure 6b), and our earlier data show that Ala + TIMP-2 suppresses eNOS activation and elevation of cytosolic cGMP levels. Given that NO directly activates sGC, this enzyme may be a target of the Ala + TIMP-2 anti-angiogenic signal. In contrast, an alternative mechanism for the Ala + TIMP-2 suppression of cGMP levels may involve activation of cGMP PDE activity. In the latter case, if PDE activation significantly contributes to the mechanism of Ala + TIMP-2 suppression of increased cGMP, inhibition of PDE activity should reverse these effects.

To evaluate this hypothesis, we measured cGMP levels in the presence of an exogenous NO donor (DETA/NO) with or without Ala + TIMP-2 after pretreatment with a non-selective phosphodiesterase inhibitor IBMX, Table 1. Pretreatment of hMVECs with IBMX, led to a 1.4-fold increase in basal level of cGMP. The cells treated with NO donors in the presence of Ala + TIMP-2 caused a 7.8-fold increase in cGMP levels while the cells treated with NO donors resulted in a 1.8-fold increase in cGMP compared with cells not treated with IBMX. Two-way ANOVA test of

Figure 6 TIMP-2 inhibits exogenous NO-induced cGMP synthesis and subsequent hMVEC proliferation and migration. (**a**) Serum-starved hMVECs were treated with 10 μM of DETA/NO (black bars) or SNAP (white bars) for 5 min. in the absence or presence of TIMP-2 (50 nM), Ala + TIMP-2 (50 nM), or ODQ (10 μM). The intracellular cGMP was determined as described in 'Materials and Methods section'. The data are presented as the mean of triplicate determinations and the results are representative of three independent experiments. *$P<0.001$ *vs* DETA/NO or SNAP in control (VEGF-A alone) cells. (**b**) hMVECs were serum starved for overnight and incubated for 24 h in the presence of the indicated concentrations of DETA/NO (black) or SNAP (grey) with (circles) or without (diamonds) Ala + TIMP-2. Cell proliferation was evaluated as described in 'Materials and Methods section'. The data are presented as the mean of triplicate determinations. *$P<0.001$ untreated *vs* DETA/NO or SNAP treated at each concentration. (**c**) hMVECs were grown to confluence and scratched in the monolayer using pipette tip. After incubation for 18 h with DETA/NO, at the indicated doses, and in the presence (grey squares) or absence (black diamonds) of Ala + TIMP-2 (50 nM), the relative migration distance of treated cells into the monolayer defect was measured. The data are presented as the mean of triplicate determinations. *$P<0.01$, **$P<0.001$ *vs* untreated (0 μM DETA/NO, in the presence of Ala + TIMP-2).

Table 1 Effects of PDE Inhibition on cGMP Levels in VEGF-A and Ala+TIMP-2-Treated hMVECs

Total cytosolic cGMP levels (pmole/mg total protein)			
	Basal	DETA/NO	Ala+TIMP-2+DETA/NO
−IBMX	1.0 ± 0.4	4.8 ± 0.07	0.8 ± 0.07
+IBMX	1.4 ± 0.03	8.5 ± 0.04	6.2 ± 0.15
Fold increase	1.4	1.8	7.8[a]

[a]Two-way ANOVA test of these data show that both the effects of the Ala+TIMP-2 treatment and the IBMX are highly significant ($P<0.001$) when compared with the control and DETA/NO alone groups.

these data show that both the effects of the Ala + TIMP-2 treatment and the IBMX are highly significant ($P<0.001$) when compared with the control and DETA/NO alone groups. These results clearly suggest that the TIMP-2-mediated signaling is capable of inducing activity of a PDE isoform. However, the identification of the specific PDE is beyond the scope of the present study.

DISCUSSION

The anti-mitogenic effects of TIMP-2 in both neoplastic and endothelial cells are independent of the ability to inhibit MMP activity.[9,11,31] Furthermore, the anti-mitogenic activity of TIMP-2 and the Ala + TIMP-2 analog are mediated by a mechanism of heterologous receptor inactivation involving the binding of Ala + TIMP-2 (or TIMP-2) to the $\alpha3\beta1$ integrin receptor enhancing PTP activity resulting in reduced activation of the cognate RTKs.[11] Murine genetic models, siRNA knockdown and biochemical experiments have been used to show the requirement for $\alpha3$ and $\beta1$ integrin subunits, and definitively identified the PTP activity as the PTP Shp-1.[11,12,31] Subsequent work demonstrated that Ala + TIMP-2 could disrupt FGF-2-mediated activation of mitogen-activated protein kinase pathway (MAPK) through an integrin $\alpha3$ and Shp-1-dependent mechanism.[10]

In this report, we have extended these studies to show that Ala + TIMP-2 suppresses maximal phosphorylation of specific tyrosine residues in the cytoplasmic domain of VEGFR-2, that diminished receptor activation is manifest in disruption of downstream signaling as evidenced by the abatement of PLC-γ activation and associated cytosolic Ca^{+2} flux, as well as curtailment of PI3K/AKT activation. We also show that Ala + TIMP-2 abates the maximal activation of eNOS and increased NO levels observed after VEGF-A stimulation, as well as the subsequent elevation of cGMP levels, associated with an enhanced mitogenesis and migration of endothelial cells. Our study also shows that Ala + TIMP-2 regulation of cGMP levels can occur independently of PTP activity via regulation of PDE activity. Although we do not analyze the precise mechanism of PDE activation, previous work from our laboratory has implicated cyclic nucleotides in TIMP-2-mediated cell growth regulation,[32] and recent work has confirmed TIMP-2 mediated elevation of cAMP levels (Seo and Stetler-Stevenson, unpublished) consistent with the differential regulation of endothelial barrier function by PDE isoforms.[33]

Ala + TIMP-2 reduced phosphorylation of selective tyrosine residues on the cytoplasmic domain of VEGFR-2. Ala + TIMP-2 suppressed maximal phosphorylation at three tyrosine residues, Y^{951}, Y^{996}, and Y^{1175}. Y^{951} and Y^{996} are located in the tyrosine kinase insert domain of VEGFR-2. Y^{951} phosphorylation results in enhanced association of this receptor with the adapter molecule VRAP/TSAd, and increases endothelial cell migration and proliferation via both PLC-γ and PI3K.[7,34] Ala + TIMP-2 also reduced phosphorylation of Y^{1175}, which is associated with the direct binding and activation of PLC-γ, as well as activation of PI3K downstream signaling pathways, both resulting in enhanced endothelial cell migration and proliferation via the MAPK pathway.[21]

Both Y^{951} and Y^{1175} of VEGFR-2 are implicated in VEGF-induced activation of eNOS, but the role of VEGFR-2 Y^{996} has not been definitively determined. The VEGFR-2 mutant $Y^{951}F$ suppresses NO release through inhibition of phosphorylation of eNOS at S^{1177}.[35] VEGFR-2 Y^{1175} mediates AKT activation, also implicated in phosphorylation of eNOS on S^{1177}.[23] In addition, PLC-γ activation through phosphorylation of Y^{1175} binding generates diacylglycerol and elevates intracellular Ca^{+2}, which as noted earlier is associated with calmodulin-mediated activation of eNOS.[25] Therefore, we speculate that Ala + TIMP-2 combined suppression of both these mechanisms cooperates to inhibit NO production. In summary, Ala + TIMP-2 suppression of maximal VEGFR-2 phosphorylation on Y^{951} and Y^{1175} effectively eliminated all of the downstream signaling effects noted above as shown either by reduced effector activity (PLC-γ, PI3K, AKT, or eNOS activity) or decreased second messenger levels (Ca^{+2} levels, NO levels, and cGMP levels), resulting in suppression of hMVEC proliferation and migration.

We have shown earlier that Ala + TIMP-2 reduced phosphoryltion of VEGFR-2, EGFR, and FGFR-1 through an increased association of Shp-1 with these receptors.[10,11,31] This led us to examine the phosphorylation of VEGFR-2 cytoplasmic tail after Ala + TIMP-2 treatment. We speculate that the specificity of this heterologous receptor inactivation mechanism of Ala + TIMP-2 inhibition of RTK phosphorylation is mediated by creation of receptor SH2-domains after activation of the receptor kinase domain. This hypothesis would explain the observation that phosphorylation of Y^{1059} on VEGFR-2 after Ala + TIMP-2 is unchanged, as this site is central for kinase activity. This finding also contrasts with a recent report describing autoregulation of VEGFR-2 phosphorylation by Shp-1 after VEGF-A binding in which Y^{1059} decreases, but Y^{951} is not effected.[36] This difference suggests that heterologous *vs* autologous down-regulation of VEGFR-2 are distinct, and one consequence is the alteration of cell motility probably regulated by Y^{951}.

In summary our present findings expand on previous reports showing that the anti-angiogenic effects of TIMP-2 involve as Shp-1-dependent mechanism of heterologous receptor inactivation. We show that Ala + TIMP-2 selectively downregulates maximal phosphorylation of VEGFR-2 on Y^{951}, Y^{996}, and Y^{1175}, with concomitant suppression of PI3K and PLC-γ signaling, resulting in abrogation of VEGF-A-stimulated hMVEC proliferation and migration. In addition, we observed that Ala + TIMP-2 enhanced activity of an IBMX-sensitive PDE that suppresses the cGMP increase after treatment with exogenous NO donors. Moreover, our results support the development of TIMP-2 as a novel, endogenous anti-angiogenic therapy that may complement those therapies already in clinical use or in preclinical trials.

ACKNOWLEDGEMENTS

We thank Drs Jensen-Taubman and Guedez for their critical reading of the paper. This study was supported by intramural research funds from the National Cancer Institute, Center for Cancer Research Project # Z01SC 009179.

DISCLOSURE/CONFLICT OF INTEREST

The authors declare no conflict interest.

1. Hanahan D, Folkman J. Patterns and emerging mechanisms of the angiogenic switch during tumorigenesis. Cell 1996;86:353–364.
2. Bergers G, Brekken R, McMahon G, *et al.* Matrix metalloproteinase-9 triggers the angiogenic switch during carcinogenesis. Nat Cell Biol 2000;2:737–744.
3. Kalluri R. Basement membranes: structure, assembly and role in tumour angiogenesis. Nat Rev Cancer 2003;3:422–433.
4. Doggrell SA. Pegaptanib: the first antiangiogenic agent approved for neovascular macular degeneration. Expert Opin Pharmacother 2005;6:1421–1423.
5. Jain RK, Duda DG, Clark JW, *et al.* Lessons from phase III clinical trials on anti-VEGF therapy for cancer. Nat Clin Pract Oncol 2006;3:24–40.
6. Regillo CD, Brown DM, Abraham P, *et al.* Randomized, double-masked, sham-controlled trial of ranibizumab for neovascular age-related macular degeneration: PIER Study year 1. Am J Ophthalmol 2008;145:239–248.
7. Olsson AK, Dimberg A, Kreuger J, *et al.* VEGF receptor signalling–in control of vascular function. Nat Rev Mol Cell Biol 2006;7:359–371.
8. Brew K, Dinakarpandian D, Nagase H. Tissue inhibitors of metalloproteinases: evolution, structure and function. Biochim Biophys Acta 2000;1477:267–283.
9. Fernandez CA, Butterfield C, Jackson G, *et al.* Structural and functional uncoupling of the enzymatic and angiogenic inhibitory activities of tissue inhibitor of metalloproteinase-2 (TIMP-2): loop 6 is a novel angiogenesis inhibitor. J Biol Chem 2003;278:40989–40995.
10. Seo DW, Kim SH, Eom SH, *et al.* TIMP-2 disrupts FGF-2-induced downstream signaling pathways. Microvasc Res 2008;76:145–151.
11. Seo DW, Li H, Guedez L, *et al.* TIMP-2 mediated inhibition of angiogenesis: an MMP-independent mechanism. Cell 2003;114: 171–180.
12. Seo DW, Li H, Qu CK, *et al.* Shp-1 mediates the antiproliferative activity of tissue inhibitor of metalloproteinase-2 in human microvascular endothelial cells. J Biol Chem 2006;281:3711–3721.
13. Shultz LD, Schweitzer PA, Rajan TV, *et al.* Mutations at the murine motheaten locus are within the hematopoietic cell protein-tyrosine phosphatase (Hcph) gene. Cell 1993;73:1445–1454.
14. Oh J, Diaz T, Wei B, *et al.* TIMP-2 upregulates RECK expression via dephosphorylation of paxillin tyrosine residues 31 and 118. Oncogene 2006;25:4230–4234.
15. Wingfield PT, Sax JK, Stahl SJ, *et al.* Biophysical and functional characterization of full-length, recombinant human tissue inhibitor of metalloproteinases-2 (TIMP-2) produced in Escherichia coli. Comparison of wild type and amino-terminal alanine appended variant with implications for the mechanism of TIMP functions. J Biol Chem 1999;274:21362–21368.
16. Lee JS, Kang Decker N, Chatterjee S, *et al.* Mechanisms of nitric oxide interplay with Rho GTPase family members in modulation of actin membrane dynamics in pericytes and fibroblasts. Am J Pathol 2005;166:1861–1870.
17. Saini R, Patel S, Saluja R, *et al.* Nitric oxide synthase localization in the rat neutrophils: immunocytochemical, molecular, and biochemical studies. J Leukoc Biol 2006;79:519–528.
18. Guo D, Tan YC, Wang D, *et al.* A Rac-cGMP signaling pathway. Cell 2007;128:341–355.
19. Dougher M, Terman BI. Autophosphorylation of KDR in the kinase domain is required for maximal VEGF-stimulated kinase activity and receptor internalization. Oncogene 1999;18:1619–1627.
20. Poulin B, Sekiya F, Rhee SG. Intramolecular interaction between phosphorylated tyrosine-783 and the C-terminal Src homology 2 domain activates phospholipase C-gamma1. Proc Natl Acad Sci USA 2005;102:4276–4281.
21. Takahashi T, Yamaguchi S, Chida K, *et al.* A single autophosphorylation site on KDR/Flk-1 is essential for VEGF-A-dependent activation of PLC-gamma and DNA synthesis in vascular endothelial cells. Embo J 2001;20:2768–2778.
22. DeBell K, Graham L, Reischl I, *et al.* Intramolecular regulation of phospholipase C-gamma1 by its C-terminal Src homology 2 domain. Mol Cell Biol 2007;27:854–863.
23. Holmqvist K, Cross MJ, Rolny C, *et al.* The adaptor protein shb binds to tyrosine 1175 in vascular endothelial growth factor (VEGF) receptor-2 and regulates VEGF-dependent cellular migration. J Biol Chem 2004;279:22267–22275.
24. Sarbassov DD, Guertin DA, Ali SM, *et al.* Phosphorylation and regulation of Akt/PKB by the rictor-mTOR complex. Science 2005;307:1098–1101.
25. Busse R, Mulsch A. Calcium-dependent nitric oxide synthesis in endothelial cytosol is mediated by calmodulin. FEBS Lett 1990;265:133–136.
26. Dimmeler S, Fleming I, Fisslthaler B, *et al.* Activation of nitric oxide synthase in endothelial cells by Akt-dependent phosphorylation. Nature 1999;399:601–605.
27. Stone JR, Marletta MA. Soluble guanylate cyclase from bovine lung: activation with nitric oxide and carbon monoxide and spectral characterization of the ferrous and ferric states. Biochemistry 1994;33:5636–5640.
28. Oh J, Seo DW, Diaz T, Wei B, Ward Y, Ray JM, *et al.* Tissue inhibitors of metalloproteinase 2 inhibits endothelial cell migration through increased expression of RECK. Cancer Res 2004;64:9062–9069.
29. Fleming I, Fisslthaler B, Dimmeler S, *et al.* Phosphorylation of Thr (495) regulates Ca(2+)/calmodulin-dependnet endothelilal nitic oxide synthetase activity. Circ Res 2001;88:E68–E75.
30. Isenberg JS, Ridnour LA, Perruccio EM, *et al.* Thrombospondin-1 inhibits endothelial cell responses to nitric oxide in a cGMP-dependent manner. Proc Natl Acad Sci USA 2005;102:13141–13146.
31. Hoegy SE, Oh HR, Corcoran ML, *et al.* Tissue inhibitor of metalloproteinases-2 (TIMP-2) suppresses TKR-growth factor signaling independent of metalloproteinase inhibition. J Biol Chem 2001;276:3203–3214.
32. Corcoran ML, Stetler-Stevenson WG. Tissue inhibitor of metalloproteinase-2 stimulates fibroblast proliferation via a cAMP-dependent mechanism. J Biol Chem 1995;270:13453–13459.
33. DeFouw LM, DeFouw DO. Differential phosphodiesterase activity contributes to restrictive endothelial barrier function during angiogenesis. Microvasc Res 2001;62:263–270.
34. Matsumoto T, Bohman S, Dixelius J, *et al.* VEGF receptor-2 Y951 signaling and a role for the adapter molecule TSAd in tumor angiogenesis. Embo J 2005;24:2342–2353.
35. Ahmad S, Hewett PW, Wang P, *et al.* Direct evidence for endothelial vascular endothelial growth factor receptor-1 function in nitric oxide-mediated angiogenesis. Circ Res 2006;99:715–722.
36. Bhattacharya R, Kwon J, Wang E, *et al.* Src homology 2 (SH2) domain containing protein tyrosine phosphatase-1 (SHP-1) dephosphorylates VEGF Receptor-2 and attenuates endothelial DNA synthesis, but not migration. J Mol Signal 2008;3:8–20.